



HAL
open science

Laguerre–Gaussian modal q-plates

Mushegh Rafayelyan, Etienne Brasselet

► **To cite this version:**

Mushegh Rafayelyan, Etienne Brasselet. Laguerre–Gaussian modal q-plates. *Optics Letters*, 2017, 42 (10), pp.1966 - 1969. 10.1364/OL.42.001966 . hal-01520388

HAL Id: hal-01520388

<https://hal.science/hal-01520388>

Submitted on 10 May 2017

HAL is a multi-disciplinary open access archive for the deposit and dissemination of scientific research documents, whether they are published or not. The documents may come from teaching and research institutions in France or abroad, or from public or private research centers.

L'archive ouverte pluridisciplinaire **HAL**, est destinée au dépôt et à la diffusion de documents scientifiques de niveau recherche, publiés ou non, émanant des établissements d'enseignement et de recherche français ou étrangers, des laboratoires publics ou privés.



Distributed under a Creative Commons Attribution - ShareAlike 4.0 International License

Laguerre–Gaussian modal q-plates

MUSHEGH RAFAYELIAN^{1,2} AND ETIENNE BRASSELET^{1,2,*}

¹Univ. Bordeaux, LOMA, UMR 5798, F-33400 Talence, France

²CNRS, LOMA, UMR 5798, F-33400 Talence, France

*Corresponding author: etienne.brasselet@u-bordeaux.fr

We propose space-variant uniaxial flat optical elements designed to generate pure Laguerre–Gaussian modes with arbitrary azimuthal and radial indices l and p from an incident Gaussian beam. This is done via the combined use of the dynamic and the geometric phases. Optimal design protocol for the mode conversion efficiency is derived, and the corresponding characteristics are given for $6 \leq l \leq 6$ and $0 \leq p \leq 5$. The obtained “modal q-plates” may find many applications whenever the radial degree of freedom of a light field is at play.

OCIS codes: (140.3300) Laser beam shaping; (050.4865) Optical vortices.

Laguerre Gaussian (LG) beams represent a well known orthogonal basis for the scalar paraxial Helmholtz equation [1], each mode being associated with a pair of indices, l and p , that correspond to two independent transverse degrees of freedom. The azimuthal index l is an integer related with the orbital angular momentum carried by a LG_{lp} beam, namely $l\hbar$ per photon along the propagation direction [2]. This property has given to the LG beams a prime position in the optics of vortex beams for 25 years. The radial index $p \geq 0$ is an integer associated with the transverse intensity distribution of the light field. Omitting the propagation factor $\exp[i(k_0 z - \omega t)]$, where k_0 is the wavenumber, z is the coordinate along the propagation direction, ω is the angular frequency, and t is the time, the complex electric field amplitude E_{lp} of a LG mode in vacuum is expressed in the cylindrical coordinate system (r, ϕ, z) as [1]

$$E_{lp}(r, \phi, z; w_0) = C_{lp} \frac{w_0}{w(z)} \left[\frac{r\sqrt{2}}{w(z)} \right]^{|l|} L_p^{|l|} \left(\frac{2r^2}{w(z)^2} \right) \exp \left[-\frac{r^2}{w(z)^2} \right] \times \exp \left\{ i \left[\frac{k_0 r^2 z}{2(z^2 + z_0^2)} + l\phi + (2p + |l| + 1) \arctan \left(\frac{z}{z_0} \right) \right] \right\}, \quad (1)$$

with C_{lp} a constant that can be derived from the beam power expression, $P = \frac{1}{2} \epsilon_0 c \int \int |E_{lp}|^2 r dr d\phi$, where ϵ_0 is the dielectric permittivity of vacuum, and c is the speed of light in vacuum. In addition, $L_p^{|l|}(x) = \sum_{k=0}^p \frac{(|l|+p)!}{(|l|+k)!(p-k)!} (-x)^k$ refers

to the associated Laguerre polynomials, w_0 is the beam waist radius, $z_0 = k_0 w_0^2 / 2$ is the Rayleigh distance, and $w(z) = w_0 \sqrt{1 + (z/z_0)^2}$.

There is a substantial gap between the studies related to the azimuthal versus radial degrees of freedom of LG beams. Nevertheless, several works have already emphasized the importance of the radial modal content. From a quantum point of view, an operator formalism for the radial modes has been established [3–5]. It has also been shown that optical information protocols may benefit from the radial degree of freedom [6–8]. The role played by the radial features of a light field within the classical picture has also been explored, for instance regarding its diffraction properties [9], but mainly in the context of the creation of pure LG modes. Contactless optical manipulation is another classical optics application example, where the superposition of LG modes including at least one high order radial mode is used to create rotating beams [10,11] or so called bottle beams [12]. In practice, numerous techniques have been introduced to produce light beams with a well defined azimuthal index l , such as diffractive optical elements [13], computer generated holograms [14], refractive spiral phase plates [15], optical cavities [16,17], or geometric phase optical elements [18], though originally restricted to the generation of LG_{l0} like vortex beams.

This has been generalized to high order radial modes with $p \geq 1$, for instance by using phase shaping via single high order diffractive optical elements [19], computer generated high order phase holograms [20], high order spiral phase plates [21], high order geometric phase optical elements [22], or amplitude only spatial light modulators [23]. Remarkably, complex amplitude modulation can be mimicked by phase only optical elements. This can be used to generate free space highly pure LG_{lp} beams [24,25] as well as other kinds of beams, for instance bounded Bessel beams or Hypergeometric beams [26]. Nevertheless, there is a practical tradeoff between accuracy and efficiency, which are competing characteristics. An intracavity high order complex amplitude modulation approach has also been developed [27]. In this context, the advent of powerful coherent integrated optical sources with controlled azimuthal and radial indices should emerge, with a huge range of practical uses in optical communications, optical imaging, optical trapping, or optical manipulation.

Here we propose another route to achieve complex amplitude modulation via the combined actions of the dynamic and geometric phases, towards the generation of pure LG modes

with arbitrary indices l and p . The dynamic phase is used to encode the desired LG field magnitude profile into one of the two circularly polarized components of the transmitted light, which is retrieved by circular polarization filtering. The geometric phase is then adjusted to provide the desired LG helical phase profile. We stress that pure LG beam shaping of one of the circularly polarized output field component is effective as soon as light emerges from the optical element. Assuming ideal polarization selection, this method thus gets rid of the tradeoff between accuracy and efficiency mentioned above.

We consider a slab of inhomogeneous anisotropic medium where both the optical axis orientation angle ψ and the birefringent phase retardation Δ are space variant in the transverse plane of the optical element with thickness L and input facet located at $z = 0$. We consider an incident circularly polarized paraxial Gaussian (LG₀₀) beam propagating along the z axis. From Eq. (1), its electric field is expressed by $\mathbf{E}_{\text{in}}(r, \phi, z < 0, t) = E_{00}(r, \phi, z; w_{0,\text{in}}) \exp[i(k_0 z - \omega t)] \mathbf{c}_\sigma$ where $\mathbf{c}_\sigma = (\mathbf{x} + i\sigma\mathbf{y})/\sqrt{2}$ with $\sigma = \pm 1$ referring to the circular polarization basis. Neglecting diffraction effects inside the slab, the output light field at $z = L$ can be straightforwardly obtained by applying locally the Jones formalism [28]. This gives for the output field, up to an unimportant phase factor $\exp[i(k_0 n_\perp L - \omega t)]$ where n_\perp (taken as constant without loss of generality) is the refractive index perpendicular to the optical axis,

$$\begin{aligned} & \mathbf{E}_{\text{out}}(r, \phi, L) \\ & \propto \exp \left[\frac{r^2}{w_{0,\text{in}}^2} + i \frac{\Delta(r, \phi)}{2} \right] \\ & \quad \times \left\{ \cos \frac{\Delta(r, \phi)}{2} \mathbf{c}_\sigma + i \sin \frac{\Delta(r, \phi)}{2} \exp[i2\sigma\psi(r, \phi)] \mathbf{c}_{-\sigma} \right\}. \end{aligned} \quad (2)$$

In the case of a uniform birefringent phase retardation $\Delta = \pi$ and azimuthally varying optical axis orientation $\psi = q\phi$ with q half integer, Eq. (2) simplifies to the known case of a “ q plate,” which refers to a pure geometric phase optical element enabling the generation of an optical vortex with polarization dependent azimuthal index $l = 2\sigma q$ [29]. However, since a q plate is imprinting a phase only modulation of the form $\exp(il\phi)$, the output light field is a superposition of a large number of LG modes with high order radial indices [30]. Our idea consists of exploiting the interplay between space variant dynamic and geometric phases in order to perform complex amplitude modulation in the circular polarization basis – specifically, by introducing appropriate radial dependence for both the birefringent phase retardation and the optical axis orientation of q plate. Namely, accounting for the structuring upgrade $\pi \rightarrow \Delta_{lp}(r)$ and $q\phi \rightarrow \psi_{lp}(r, \phi)$, here after we demonstrate that pure LG _{lp} modes can be generated.

Such a “modal q plate” produces a σ polarized LG _{lp} beam if the following condition is satisfied:

$$\mathbf{E}_{\text{out}}(r, \phi, L) \cdot \mathbf{c}_{-\sigma}^* \propto E_{lp}(r, \phi, 0; w_{0,\text{out}}), \quad (3)$$

where the asterisk denotes complex conjugation. The corresponding expressions for $\Delta_{p,l}$ and $\psi_{p,l}$ are derived from Eqs. (1) and (2):

$$\Delta_{lp}(r) = 2 \arcsin \left(\frac{|E_{lp}(r; w_{0,\text{out}}) \exp(r^2/w_{0,\text{out}}^2)|}{\max_r[|E_{lp}(r; w_{0,\text{out}}) \exp(r^2/w_{0,\text{out}}^2)|]} \right), \quad (4)$$

which implies that the ratio $\zeta = w_{0,\text{out}}/w_{0,\text{in}}$ between the waist radius w_0 of the LG _{lp} mode and that of the incident Gaussian

beam satisfies $0 \leq \zeta \leq 1$ in order to ensure a finite value for the $\max_r[\cdot]$ operator, and

$$\psi_{lp}(r, \phi) = \frac{\sigma}{2} \left(l\phi - \frac{\Delta_{lp}(r)}{2} \right) - \frac{\pi}{2} \left(1 - H \left[L_p^{|l|} \left(\frac{2r^2}{w_{0,\text{out}}^2} \right) \right] \right), \quad (5)$$

where we introduced the unit step function defined as $H(x \leq 0) = 0$ and $H(x > 0) = 1$. By doing so, the birefringent phase retardation is always positive and transforms the incident Gaussian intensity profile into that of the desired LG _{lp} mode while the optical axis orientation profile ensures a purely helical wavefront at the output of the modal q plate.

As expected from the Laguerre Gaussian apodization of the incident Gaussian beam, only a fraction η of the incident power is transformed into a given LG _{lp} mode. From Eq. (2), and accounting that $\int_0^\infty \exp(-2r^2/w_{0,\text{in}}^2) r dr = w_{0,\text{in}}^2/4$, the modal efficiency is thus expressed as

$$\eta_{lp} = \frac{4}{w_{0,\text{in}}^2} \int_0^\infty \sin^2[\Delta_{lp}(r, \phi)/2] \exp(-2r^2/w_{0,\text{in}}^2) r dr. \quad (6)$$

From Eqs. (4) and (6), it can be shown that η_{lp} depends only on the waists ratio ζ ; see Fig. 1 for $1 \leq l \leq 3$ and $0 \leq p \leq 2$. The optimal value ζ_{lp}^{opt} that maximizes the modal efficiency $\eta_{lp}^{\text{opt}} = \eta_{lp}(\zeta_{lp}^{\text{opt}})$, and the latter value itself, both depend on l and p . The results are summarized in Tables 1 and 2 for $6 \leq l \leq 6$ and $0 \leq p \leq 5$.

Interestingly, the modal problem has a simple analytical solution when $p = 0$. Indeed, in that case, Eqs. (4)–(6) are respectively expressed as

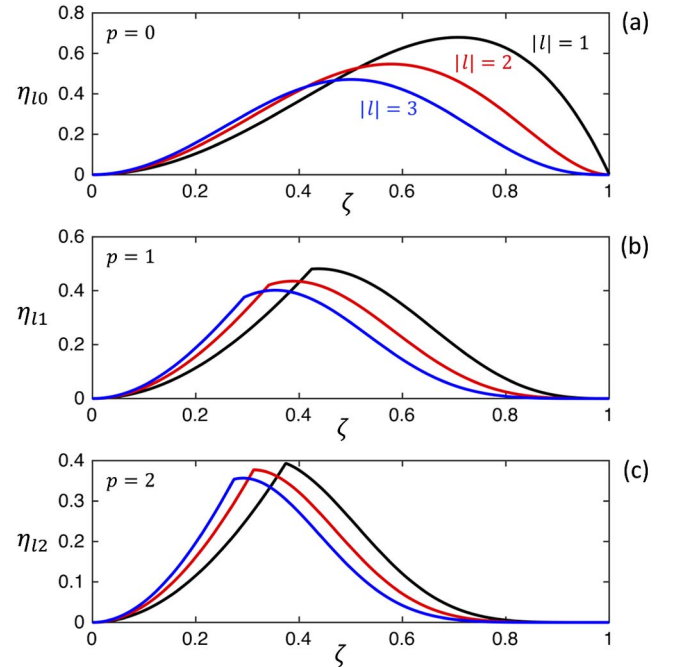


Fig. 1. Modal q plate efficiency as a function of the reduced LG _{lp} beam waist $w_{0,\text{out}}/w_{0,\text{in}}$ for $|l| = 1$ (black curves), $|l| = 2$ (red curves), and $|l| = 3$ (blue curves), in the case $p = 0$ [panel (a)], $p = 1$ [panel (b)], and $p = 2$ [panel (c)].

Table 1. Optimal Values ζ_{lp}^{opt} Maximizing η_{lp} for $-6 \leq l \leq 6$ and $0 \leq p \leq 5$

	$ l = 1$	$ l = 2$	$ l = 3$	$ l = 4$	$ l = 5$	$ l = 6$
$p = 0$	0.71	0.58	0.50	0.45	0.41	0.38
$p = 1$	0.44	0.39	0.35	0.33	0.31	0.29
$p = 2$	0.38	0.32	0.29	0.27	0.26	0.25
$p = 3$	0.34	0.29	0.26	0.24	0.23	0.22
$p = 4$	0.32	0.27	0.25	0.23	0.21	0.20
$p = 5$	0.30	0.26	0.24	0.22	0.20	0.19

Table 2. Optimal Values η_{lp}^{opt} of the Modal Q -Plate Efficiency for $-6 \leq l \leq 6$ and $0 \leq p \leq 5$

	$ l = 1$	$ l = 2$	$ l = 3$	$ l = 4$	$ l = 5$	$ l = 6$
$p = 0$	0.68	0.55	0.47	0.42	0.38	0.35
$p = 1$	0.48	0.44	0.40	0.38	0.35	0.34
$p = 2$	0.39	0.38	0.36	0.34	0.33	0.31
$p = 3$	0.33	0.34	0.34	0.31	0.30	0.29
$p = 4$	0.29	0.30	0.30	0.29	0.29	0.28
$p = 5$	0.25	0.27	0.28	0.27	0.27	0.27

$$\Delta_{l0}(r) = 2 \arcsin \left[\left(\sqrt{\frac{2}{|l|}} \frac{r}{W} \right)^{|l|} \exp \left(\frac{r^2}{W^2} + \frac{|l|}{2} \right) \right], \quad (7)$$

$$\psi_{l0}(r, \phi) = \frac{\sigma}{2} \left(l\phi - \frac{\Delta_{l0}(r)}{2} \right), \quad (8)$$

$$\eta_{l0} = \zeta^2 |l|! \left[\frac{e}{|l|} (1 - \zeta^2) \right]^{|l|}, \quad (9)$$

where we have introduced the effective waist radius

$$W = w_{0,\text{in}} \frac{\zeta}{\sqrt{1 - \zeta^2}}. \quad (10)$$

This gives the following expressions for the parameters of optimal modal q plates:

$$\zeta_{l0}^{\text{opt}} = \frac{1}{\sqrt{1 + |l|}}, \quad (11)$$

$$\eta_{l0}^{\text{opt}} = \frac{|l|! e^{|l|}}{(1 + |l|)^{1+|l|}}. \quad (12)$$

For the sake of illustration, the maps of the optimal birefringence phase retardation $\Delta_{lp}^{\text{opt}}(r)$ and optical axis orientation angle $\psi_{lp}^{\text{opt}}(r, \phi)$ are shown in Figs. 2 and 3 for $3 \leq l \leq 3$ and $0 \leq p \leq 2$. The visual inspection of these maps allows grasping the fabrication challenge towards the practical realization of modal q plates. Indeed, to date, the various technologies used to engineer q plates are basically implemented within a scheme of planar slabs exhibiting a constant birefringent phase retardation. For instance, one can mention liquid crystals [31] or polymer liquid crystals [32] photoalignment technologies that deal with the structuring of truly birefringent media. There are also strategies based on form birefringent media, where the effective optical anisotropy emerges from subwavelength structuring of isotropic materials, such as femtosecond laser structuring of glasses [33] or polymers [34], nanofabrication enabled structuring of metals [35] or dielectrics [36]. In the former case, it is very challenging to consider the independent local control

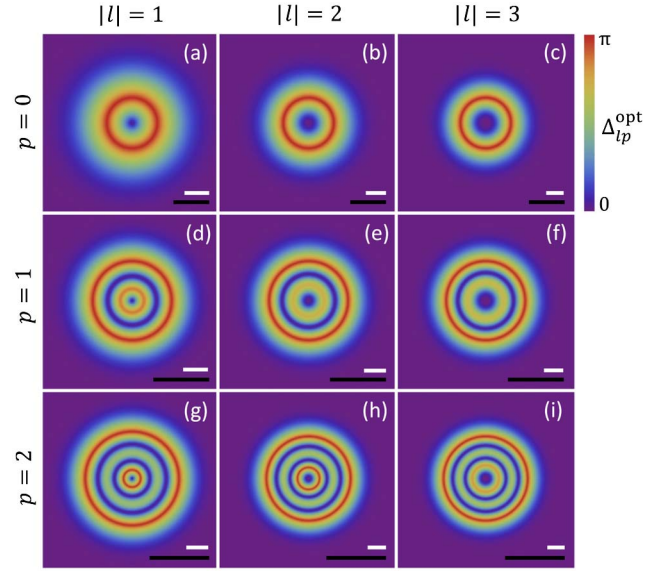


Fig. 2. In plane spatial distribution of the birefringent phase retardation $\Delta_{lp}^{\text{opt}}(r)$ of optimal modal q plates for $3 \leq l \leq 3$ and $0 \leq p \leq 2$. White scale bar: $w_{0,\text{out}}$. Black scale bar: $w_{0,\text{in}}$.

of both the birefringent phase retardation and the optical axis orientation, although arbitrary in plane optical axis patterns at fixed retardance can nowadays be achieved [37]. In the latter case, however, one could consider retardance control at fixed structured thickness via space variant filling factor $F(r, \phi)$ of a given subwavelength step grating of period Λ , each period consisting of a $F\Lambda$ width with refractive index n_1 and a $(1 - F)\Lambda$ width with refractive index n_2 , which lead to an effective birefringence dn that depends on n_1 , n_2 , and F . By doing so, an arbitrary pattern $\Delta(r, \phi)$ can be obtained from the relationship $\Delta(r, \phi) = \frac{2\pi}{\lambda} dn(n_1, n_2, F(r, \phi))L$. Another

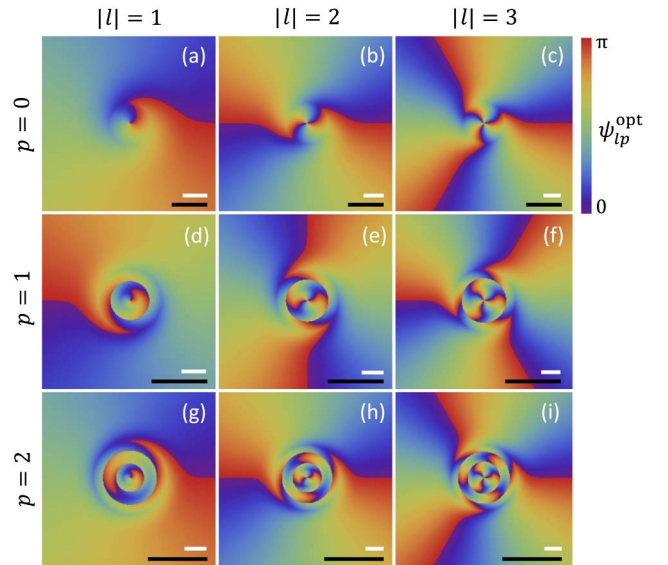


Fig. 3. In plane spatial distribution of the optical axis orientation angle $\psi_{lp}^{\text{opt}}(r, \phi)$ of optimal modal q plates for $3 \leq l \leq 3$ and $0 \leq p \leq 2$. White scale bar: $w_{0,\text{out}}$. Black scale bar: $w_{0,\text{in}}$.

solid state option could rely on the use of space variant antennas designed to control the complex amplitude of light. In other words, the practical realization of modal q plates is accessible to state of the art nanofabrication tools.

In addition, self engineered strategies that do not rely on machining techniques can also be considered. Indeed, it has been shown that various kinds of spontaneously formed liquid crystal defect structures enable the generation of an optical vortex beam with spin controlled azimuthal index with the additional key feature demonstrated here, namely $\Delta = \Delta(r)$ with $\Delta(0) = 0$. One can mention hedgehog defects [38], umbilics [39] and disclinations [40] in nematics, focal conic domains in smectics [41], and solitonic defect structures in cholesterics [42]. Moreover, liquid crystals are natural candidates for the required twisted configurations of the form $\psi(r, \phi) = l\phi + f(r)$, one shown for instance in the case of nematic films under all optical [43] or electro optical [44] external stimuli. That is to say, the engineering of modal q plates could also be considered using soft matter optically anisotropic systems.

Recalling that the usual q plates have already found a lot of applications both in classical and quantum optics [45] and are likely to find many others in the future [46], modal q plates enabling the control of both the azimuthal and radial modal content of a light field with a single optical element, possibly integrated [47], should be of interest in many scientific and technological areas. It should be mentioned that modal q plates are designed for a given azimuthal index l that cannot be switched to $-l$ by mere flip of the helicity of the incident light field, but flipping also the optical element along the propagation axis. Finally, we note that the proposed combined action of dynamic and geometrical phases towards the control of the radial degree of freedom of a light field represents another attempt to tailor the spatial properties of electromagnetic fields by hybrid phase transformations [48,49].

Funding. Agence Nationale de la Recherche (ANR) (ANR 15 CE30 0018).

REFERENCES

1. A. E. Siegman, *Lasers* (University Science Books, 1986).
2. L. Allen, M. W. Beijersbergen, R. J. C. Spreeuw, and J. P. Woerdman, *Phys. Rev. A* **45**, 8185 (1992).
3. E. Karimi and E. Santamato, *Opt. Lett.* **37**, 2484 (2012).
4. E. Karimi, R. Boyd, P. de la Hoz, H. de Guise, J. Řeháček, Z. Hradil, A. Aiello, G. Leuchs, and L. L. Sánchez Soto, *Phys. Rev. A* **89**, 063813 (2014).
5. W. N. Plick and M. Krenn, *Phys. Rev. A* **92**, 063841 (2015).
6. Y. Zhang, F. S. Roux, M. McLaren, and A. Forbes, *Phys. Rev. A* **89**, 043820 (2014).
7. E. Karimi, D. Giovannini, E. Bolduc, N. Bent, F. M. Miatto, M. J. Padgett, and R. W. Boyd, *Phys. Rev. A* **89**, 013829 (2014).
8. M. Krenn, M. Huber, R. Fickler, R. Lapkiewicz, S. Ramelow, and A. Zeilinger, *Proc. Natl. Acad. Sci. USA* **111**, 6243 (2014).
9. J. Mendoza Hernández, M. L. Arroyo Carrasco, M. D. Iturbe Castillo, and S. Chávez Cerda, *Opt. Lett.* **40**, 3739 (2015).
10. S. N. Khonina, V. V. Kotlyar, V. A. Soifer, M. Honkanen, J. Lautanen, and J. Turunen, *J. Mod. Opt.* **46**, 227 (1999).
11. S. Franke Arnold, J. Leach, M. J. Padgett, V. E. Lembessis, D. Ellinas, A. J. Wright, J. M. Girkin, P. Ohberg, and A. S. Arnold, *Opt. Express* **46**, 227 (2007).
12. J. Arit and M. J. Padgett, *Opt. Lett.* **25**, 191 (2000).
13. V. Y. Bazhenov, M. Vasnetsov, and M. Soskin, *JETP Lett.* **52**, 429 (1990).
14. N. Heckenberg, R. McDuff, C. Smith, and A. White, *Opt. Lett.* **17**, 221 (1992).
15. S. Khonina, V. Kotlyar, M. Shinkaryev, V. Soifer, and G. Uspleniev, *J. Mod. Opt.* **39**, 1147 (1992).
16. M. Harris, C. Hill, P. Tapster, and J. Vaughan, *Phys. Rev. A* **49**, 3119 (1994).
17. S. C. Chu and K. Otsuka, *Opt. Commun.* **281**, 1647 (2008).
18. G. Biener, A. Niv, V. Kleiner, and E. Hasman, *Opt. Lett.* **27**, 1875 (2002).
19. S. Khonina, V. V. Kotlyar, R. Skidanov, V. Soifer, P. Laakkonen, and J. Turunen, *Opt. Commun.* **175**, 301 (2000).
20. Y. Ohtake, T. Ando, N. Fukuchi, N. Matsumoto, H. Ito, and T. Hara, *Opt. Lett.* **32**, 1411 (2007).
21. G. Ruffato, M. Massari, and F. Romanato, *Opt. Lett.* **39**, 5094 (2014).
22. P. Chen, B. Y. Wei, W. Ji, S. J. Ge, W. Hu, F. Xu, V. Chigrinov, and Y. Q. Lu, *Photon. Res.* **3**, 133 (2015).
23. V. Lerner, D. Shwa, Y. Drori, and N. Katz, *Opt. Lett.* **37**, 4826 (2012).
24. V. Arrizón, U. Ruiz, R. Carrada, and L. A. González, *J. Opt. Soc. Am. A* **24**, 3500 (2007).
25. T. Ando, Y. Ohtake, N. Matsumoto, T. Inoue, and N. Fukuchi, *Opt. Lett.* **34**, 34 (2009).
26. S. N. Khonina, S. A. Balalayev, R. Skidanov, V. V. Kotlyar, B. Paivanranta, and J. Turunen, *J. Opt. A* **11**, 065702 (2009).
27. S. Ngcobo, I. Litvin, L. Burger, and A. Forbes, *Nat. Commun.* **4**, 2289 (2013).
28. E. Brasselet, *Opt. Lett.* **38**, 3890 (2013). In that paper, the misprint “q integer” should be replaced by “q half integer.”
29. L. Marrucci, C. Manzo, and D. Paparo, *Phys. Rev. Lett.* **96**, 163905 (2006).
30. A. Forbes, A. Dudley, and M. McLaren, *Adv. Opt. Photon.* **8**, 200 (2016).
31. S. Slussarenko, A. Murauski, T. Du, V. Chigrinov, L. Marrucci, and E. Santamato, *Opt. Express* **19**, 4085 (2011).
32. S. R. Nersisyan, N. V. Tabiryan, D. Mawet, and E. Serabyn, *Opt. Express* **21**, 8205 (2013).
33. M. Beresna, M. Gecevičius, P. G. Kazansky, and T. Gertus, *Appl. Phys. Lett.* **98**, 201101 (2011).
34. X. Wang, A. Kuchmizhak, E. Brasselet, and S. Juodkazis, “Dielectric geometric phase optical elements from femtosecond direct laser writing,” arXiv:1612.04487 (2016).
35. D. Hakobyan, H. Magallanes, G. Seniutinas, S. Juodkazis, and E. Brasselet, *Adv. Opt. Mater.* **4**, 306 (2016).
36. R. C. Devlin, A. Ambrosio, D. Wintz, S. L. Oscurato, A. Y. Zhu, M. Khorasaninejad, J. Oh, P. Maddalena, and F. Capasso, *Opt. Express* **25**, 377 (2017).
37. J. Kim, Y. Li, M. N. Miskiewicz, C. Oh, M. W. Kudenov, and M. J. Escuti, *Optica* **2**, 958 (2015).
38. E. Brasselet, N. Murazawa, H. Misawa, and S. Juodkazis, *Phys. Rev. Lett.* **103**, 103903 (2009).
39. E. Brasselet and C. Loussert, *Opt. Lett.* **36**, 719 (2011).
40. C. Loussert, U. Delabre, and E. Brasselet, *Phys. Rev. Lett.* **111**, 037802 (2013).
41. B. Son, S. Kim, Y. H. Kim, K. Käläläntär, H. M. Kim, H. S. Jeong, S. Q. Choi, J. Shin, H. T. Jung, and Y. H. Lee, *Opt. Express* **22**, 4699 (2014).
42. B. Yang and E. Brasselet, *J. Opt.* **15**, 044021 (2013).
43. E. Brasselet, *Opt. Lett.* **34**, 3229 (2009).
44. R. Barboza, U. Bortolozzo, M. G. Clerc, S. Residori, and E. Vidal Henríquez, *Philos. Trans. R. Soc. A* **372**, 20140019 (2014).
45. L. Marrucci, E. Karimi, S. Slussarenko, B. Piccirillo, E. Santamato, E. Nagali, and F. Sciarino, *J. Opt.* **13**, 064001 (2011).
46. L. Marrucci, *J. Nanophoton.* **7**, 078598 (2013).
47. M. S. Seghilani, M. Myara, M. Sellahi, L. Legratiet, I. Sagnes, G. Beaudoin, P. Lalanne, and A. Garnache, *Sci. Rep.* **6**, 38156 (2016).
48. M. Pal, C. Banerjee, S. Chandell, A. Bag, S. K. Majumder, and N. Ghosh, *Sci. Rep.* **6**, 39582 (2016).
49. Z. Liu, Y. Liu, Y. Ke, Y. Liu, W. Shu, H. Luo, and S. Wen, *Photon. Res.* **5**, 15 (2017).